

Vascularization of Microfluidic Hydrogels

8

8.1 Introduction

Current methods for engineering vascularized tissues rely primarily on the self-organization of vascular cells (endothelial cells, pericytes, and smooth muscle cells) or their progenitors in a scaffold and/or on the recruitment of new vessels via release of angiogenic factors [1,2]. While these approaches certainly accelerate the process of graft vascularization, they still require several days to achieve perfusion of the graft. It is difficult to see how thick, densely cellularized grafts (e.g., a myocardial patch) could survive the stagnant transition period that separates *in vitro* culture from *in vivo* perfusion.

In clinical tissue transplantation, grafted tissues are almost always (re)perfused upon completion of the surgical procedure. For instance, successful transfer of a “free flap” between distant regions of the human body requires microvascular anastomoses between the small vessels that feed the tissue and those that reside in the recipient bed [3]. Insetting the graft without establishing such anastomoses usually leads to necrosis of the graft (with the exception of thin tissues such as epidermal grafts).

These issues have prompted us and others to investigate how to create tissues that can be immediately perfused. Our approach is to form scaffolds that contain microfluidic networks that serve both as channels for perfusion and as templates for vascular growth [4–6]. We emphasize that such an approach differs from the “prevascularization” that often results in organization of vascular cells into short segments that have not been shown to sustain flow across the entire scaffold [7,8]. This chapter describes methods to form, vascularize, and optimize microfluidic scaffolds for perfusion of engineered tissues, and proposes a computational algorithm to simplify the design of microfluidic scaffolds for this application.

8.2 Design criteria for microfluidic scaffolds

What basic features should microfluidic scaffolds possess? First, the channels in these scaffolds must span the entire dimension of the scaffold. In this way, application of a pressure difference across the scaffold can lead to flow within the

channels. Although flow is possible even in the absence of channels (since scaffolds are generally porous), such interstitial flows appear to be limited to the *in vitro* setting; to maintain nutritive flows, they require large pressure gradients and generate large interstitial shear stresses [9]. Second, the channels should have dimensions appropriate for the vascular system. Given that we envision eventually perfusing these scaffolds with blood or with a suspension of red blood cells, it would not make sense to design channels narrower than $\sim 5 \mu\text{m}$. Third, the scaffolds must promote adhesion and spreading of vascular cells, as we intend to form vessels within the channels. As noted in subsequent sections, the adhesion strength between cells and scaffold channels will affect the design of the microfluidic geometry. Fourth, the scaffold must be able to support passive diffusion of oxygen and solutes from the channel to cells embedded within the scaffold, as well as resist the mechanical stresses induced by perfusion. In particular, the scaffold must not have such a small pore size that it restricts the transport of serum proteins.

We have chosen to make microfluidic scaffolds from hydrogels of extracellular matrix (ECM) proteins, chiefly, type I collagen and fibrinogen. These materials are inherently adhesive to vascular cells, promote the formation of endothelium, and can have pore sizes greater than the sizes of most proteins. By learning how to build microfluidic networks in these materials and how to vascularize the networks, we hope to uncover broad principles that can be applied to the vascularization of non-ECM-based materials.

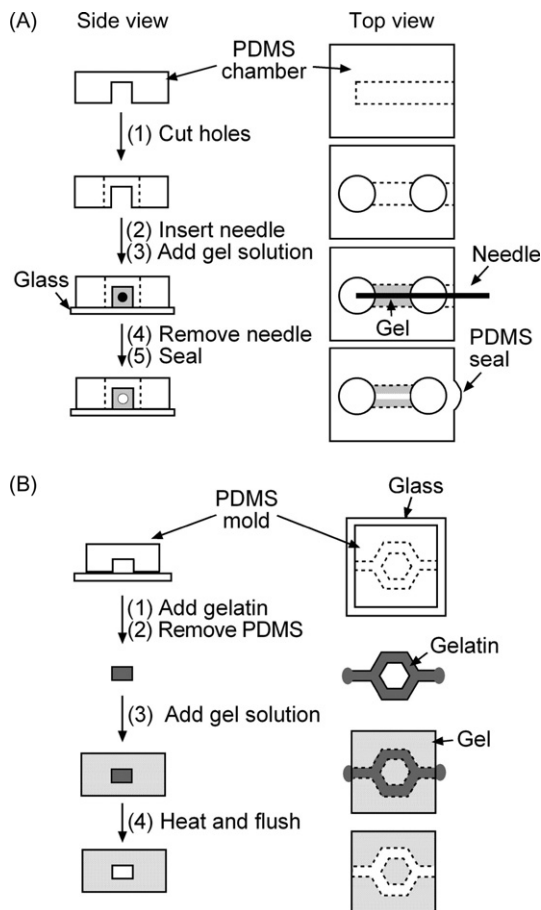
8.3 Forming and vascularizing microfluidic gels

8.3.1 Forming microfluidic gels

We have taken two approaches to form microfluidic ECM gels. The first one is subtractive, in which a channel forms when a sacrificial material is removed from the gel. Examples include the removal of a cylindrical template to form a single channel, and the dissolution of a micromolded gelatin mesh to form a network [5,10]. The second approach is additive, in which the irreversible adhesion of two gels into a monolithic whole can result in the formation of channels [6]. Both approaches are applicable to a wide variety of materials, although we have used them primarily in ECM gels.

8.3.1.1 Subtractive methods

To form ECM gels that contain single channels, we have used thin stainless steel needles as removable templates (Figure 8.1A) [10,11]. The needles are typically $\sim 120 \mu\text{m}$ in diameter (we use 02 Japanese gauge acupuncture needles); to obtain narrower needles, we etch them for a few minutes in a nickel etchant. We then adsorb a layer of bovine serum albumin (BSA) onto the needles to prevent gels from adhering to them [12]. We finally introduce liquid gel precursor around the

**FIGURE 8.1**

(A) Needle-based method to form a single channel. (B) Gelatin-based method to form a network of channels.

Source: Modified from Refs. [5,10] with permission from Elsevier and the Royal Society of Chemistry.

BSA-coated needles, taking care that both ends of a needle are left uncovered. Gelation, followed by removal of a needle, yields a gel that contains a channel of the same diameter as the needle.

In practice, various external aids are required to obtain a well-formed channel. The ECM gels that we use can be quite soft and hence can be easy to deform irreversibly. We typically restrain the gels within a mechanical support, so that the gels do not shift during removal of a needle. Likewise, we use a guide to eliminate vibrations and lateral movement of the needle during its

removal. With these precautions, this procedure can routinely make open channels as narrow as $\sim 50\ \mu\text{m}$. Although it is possible to form narrower channels by using thinner needles, we have found that vascularizing such channels is difficult (see Section 8.3.2).

By arranging needles in arrays (either side-by-side or atop each other), it is possible to form gels that contain parallel arrays of channels. Such a configuration mimics the hexagonal vascular geometry analyzed by the physiologist Krogh [13], and its regularity allows for computational models and/or analytical expressions that describe its transport properties (see Section 8.4). These arrays appear to be well suited for perfusing constructs *in vitro*. Because they contain numerous inlets and outlets (one pair per channel), however, it is currently impractical to use them as vascular templates for microsurgical grafting.

To obtain greater versatility in the arrangement of channels within microfluidic gels, we have developed a subtractive lithographic method to replicate patterns inside ECM gels (Figure 8.1B) [5]. The subtractive element in this method is a molded gelatin mesh. We typically generate these meshes by thermosetting concentrated gelatin solutions within standard silicone polydimethylsiloxane (PDMS)-based microfluidic networks. Other methods for making gelatin microstructures (e.g., molding within hollow fibers) are possible, although they lack the versatility of a lithographic approach in the types of patterns generated (Golden and Tien, unpublished data). As with the needles described earlier, we encapsulate the gelatin meshes in ECM gels (taking care to leave the ends free). Since gelatin gels melt at 37°C , heating the encapsulated gels and imposing a pressure gradient across the ECM gel removes the molded structure, leaving behind microfluidic channels that replicate the geometry of the mesh. We have found that gelatin swells noticeably (by 20–40%, depending on preparation conditions), so it is important to design narrower meshes to obtain channels of the desired widths.

The strength and flexibility of gelatin meshes provide interesting opportunities to build thick microfluidic scaffolds. Meshes can be stacked or folded to form overlapping networks that span a thicker volume [5]. Because the lithographic procedure generates two-dimensional (2D) networks, stacked or folded meshes cannot reproduce the highly interconnected three-dimensional (3D) geometries characteristic of vascular beds *in vivo*. Nevertheless, using meshes that possess a treelike network geometry can greatly reduce the number of inlets and outlets in a microfluidic scaffold, which makes microsurgical implantation more plausible.

8.3.1.2 Additive methods

We have also developed an additive procedure to form microfluidic scaffolds [6]. We based this method on the procedures previously developed for forming 3D networks in PDMS devices, in which stacking and bonding of planar PDMS layers led to layer-by-layer construction of a 3D structure [14]. Unlike PDMS, however, hydrogels do not seal tightly to each other; in fact, even the modest forces exerted by living cells are sufficient to pry apart passively adherent gels. Thus, we identified compounds that could be used to bond gels irreversibly.

These compounds were “perturbants” that, if added at sufficiently high concentration, would dissolve the gels. At a subthreshold concentration, perturbants partially solubilize gels and generate locally high concentrations of gel monomer. Upon removal of the perturbant, the gel monomers repolymerize to “glue” passively adherent gels together. Examples of gel-bonding solutes include classical chaotropes such as urea and guanidine, as well as ECM-specific ones such as glycerol (for type I collagen). In practice, we mold gels so that two of them would form a microfluidic network when placed in contact. Addition and removal of perturbant occur by perfusion through these networks.

In principle, this bonding procedure can be applied iteratively to form 3D networks in gels, much as is currently done in PDMS. The practical difficulties in aligning patterned soft gels across large areas, however, have limited its application to date to 2D networks [6].

8.3.2 Vascularizing gels

8.3.2.1 Basic concepts

To use the barren channels in a microfluidic scaffold as templates for the formation of vessels, we introduce suspensions of vascular cells (endothelial cells in most studies, although we have examined cocultures of endothelial and mesenchymal cells) by perfusion [10,15]. As long as the cells do not clog the channels, they will adhere, spread, and proliferate within the channels. Channels of diameter $\geq 100\ \mu\text{m}$ can be seeded routinely; with practice, those of diameter $\geq 50\ \mu\text{m}$ can also be seeded. In channels narrower than $50\ \mu\text{m}$, clogs invariably form, and these channels can only be vascularized by promoting migration from adjacent larger vessels (Price and Tien, unpublished results). Once channels are seeded, we place them under a pressure difference to induce flow. To maintain the pressure head, we find that manually recirculating the perfusion media is sufficient.

Cells from large vessels (e.g., umbilical vein) and from microvessels are both suitable for vascularization of microfluidic scaffolds, although subtle differences exist in the final structures. In all cases, endothelial cells settle and adhere preferentially to the lower surface of channels. Over the next 1–2 days, the cells migrate along the channel and proliferate to form confluent lumens. The lumens never occlude over time. In vessels made from human umbilical vein endothelial cells, the endothelium initially aligns parallel to the direction of flow; in vessels of human dermal microvascular endothelial cells, the endothelium does not align in any direction under flow.

Vascularization of cylindrical channels leads, not surprisingly, to vessels that have cylindrical lumens [10]. Vascularization of channels that have rectangular cross sections (e.g., scaffolds made by gelatin- or perturbant-based lithographic methods) yield vessels that have rounded lumens, at least in the soft ECM gels we have tested. We believe that the inherent contractility of the seeded cells is partly responsible for generating a surface tension that leads to stress concentration at the sharp edges of the channels and subsequent rounding of the channel shape.

8.3.2.2 Promoting vascular stability and function

Although the open structure of vascularized channels supports initial perfusion, we have found that long-term perfusion is not guaranteed. That is, the microfluidic nature of a scaffold is necessary, but not sufficient, to allow immediate and sustained perfusion. The endothelium is responsible for changes in perfusion, since barren channels can be perfused essentially without limit. The many ways in which endothelium can disrupt the channel profile and thereby alter the flow resistance include: contracting the scaffold, invading the scaffold, and delaminating from the scaffold [10,16,17]. Contraction and invasion typically occur within a few days postseeding, whereas delamination can present over several days.

These changes can be limited, in part, by altering the bulk physical properties of the scaffold [10]. Scaffold contraction results from competition between the cellular contractility and the gel stiffness. We have found that scaffolds of shear modulus of at least several hundred Pascal are rigid enough to resist deformation. Invasion of the scaffold, however, correlates with scaffold porosity. Scaffolds with Darcy permeabilities of at most $\sim 0.1 \mu\text{m}^2$ are nonporous enough to resist invasion. In practice, both of these requirements are met in 6–10 mg/ml type I collagen gels that are formed at pH 7–7.5 and $\leq 25^\circ\text{C}$.

To understand how to limit endothelial delamination (and thus enable stable long-term perfusion), we have considered the forces and flows within vascularized microfluidic scaffolds in the presence of perfusion [16,17]. In particular, we have proposed that a balance of forces exists at the interface between the endothelium and the channel surface [16]; for stable vessels, the following inequality must hold:

$$\sigma_{\text{adh}} + P_t > \frac{\gamma_{\text{EC}}}{R} \quad (8.1)$$

Here, the interfacial adhesion stress σ_{adh} promotes vascular stability, as does transmural pressure P_t (defined as perfusion pressure in the lumen minus interstitial pressure in the scaffold). Endothelial contractility γ_{EC} induces a destabilizing stress that is inversely proportional to channel radius R . This hypothesis assumes that the delamination that we have observed is purely physical in origin (e.g., is independent of proteases). It predicts that modulation of endothelial contractility and/or perfusion stresses can enhance stability, as described below; we have not investigated altering the adhesivity of the scaffold surface.

8.3.2.3 Modulation of intravascular cyclic adenosine monophosphate (AMP)

It is well known from studies of endothelial cells that endothelial contractility results from activation of the actomyosin filament [18]. Here, the second messenger cyclic AMP (cAMP) serves to “relax” endothelial cells by activating protein kinase A, which phosphorylates the GTPase RhoA, and thus inhibits generation of tension [19]; nonclassical relaxation mechanisms that bypass protein kinase A also exist [20,21]. We have thus investigated to what extent elevation of cAMP levels could stabilize vessels in microfluidic scaffolds [16]. Since the cell

membrane is impermeable to cAMP, we used an esterified analog (dibutryl cAMP) and a phosphodiesterase inhibitor (Ro-20-1724); these compounds were added directly to the perfusate. As expected, addition of cAMP-elevating compounds led both to decreased contractility (as measured by radial strain of the lumen) (Figure 8.2A) and increased stability (Figure 8.2B). At the highest concentrations of dibutryl cAMP (400 μM) with Ro-20-1724 (20 μM), vessels did not delaminate over the span of 2 weeks; the longest we have kept vessels under these conditions is ~ 2 months.

Strangely, the dose-dependence of reduced contractility and increased vascular stability did not match. Whereas the loss of contractility required the highest concentrations of cAMP-elevating compounds, stabilization was already apparent at lower concentrations of dibutryl cAMP (80 μM). Thus, loss of contractility is not necessary for stabilization.

To determine if other effects of elevated cAMP levels might stabilize vessels, we examined the barrier function and turnover rates. Time-lapse videos of the efflux of fluorescent solutes from the perfusate into the scaffold revealed that the vessels were extremely leaky in the absence of cAMP-elevating agents (Figure 8.2C). Addition of moderate concentrations of dibutryl cAMP (80 μM) was sufficient to largely eliminate these leaks. Turnover rates in the absence of cAMP-elevating compounds were small and consistent with the nonzero proliferation rates observed in postconfluent endothelium in culture. Only in the presence of high concentrations of cAMP-elevating compounds did the turnover rates decrease to essentially zero. These dose-dependences suggest that leaks may destabilize vessels in microfluidic scaffolds, whereas cell turnover (which itself can induce leaks [22,23]) is not a major factor. Indeed, computational models of the pressure profile within the scaffold near a leak showed that a leak allowed luminal pressure to “diffuse” into the scaffold, thereby elevating scaffold pressure and reducing transmural pressure. These models indicated that the large numerous leaks observed in the absence of cAMP-elevating compounds resulted in a loss of 1–2 cm H_2O of stabilizing transmural pressure, which may be sufficient to induce delamination of the endothelium from the scaffold wall.

8.3.2.4 Modulation of perfusion stresses

We have also investigated to what extent changes in perfusion stresses affect vascular stability [17]. Our original motivation for these studies was to understand an early observation that vessels under higher flow invariably sustained perfusion for a longer period. As seen with cAMP-mediated stabilization, flow-induced stabilization was accompanied by elimination of leaks from the vessel wall (Figure 8.2D). The same mechanism of stabilization (loss of leaks to increase transmural pressure) appears to apply whether flow or cAMP levels are increased.

To elucidate the detailed mechanism behind flow-induced stabilization, we considered the stresses induced by flow. We calculated that increases in flow rate resulted in simultaneous increases in average luminal pressure, shear stress, and transmural pressure. By altering luminal pressures without changing flow rate,

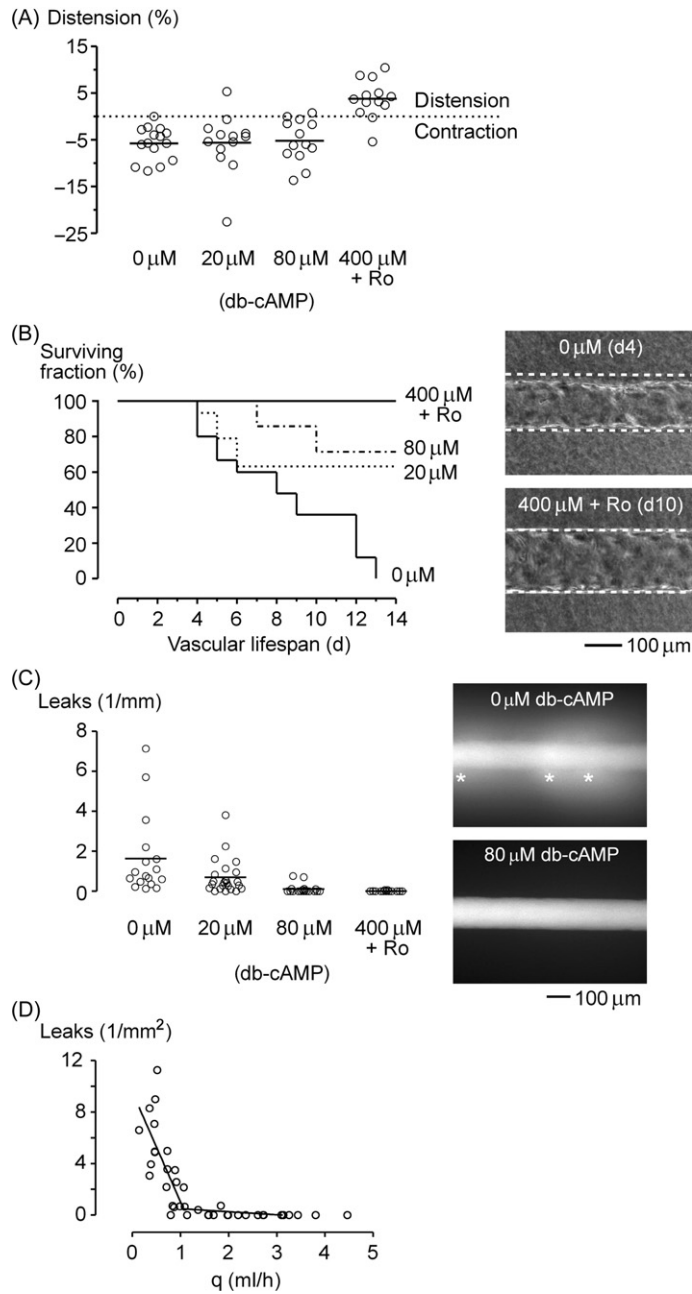


FIGURE 8.2

(A) Increases in cAMP levels reduce or reverse contractility of the vessel wall.

(B) Increases in cAMP levels prevent endothelial delamination and prolong lifespan of the

(Continued)

we found that the vascular phenotype did not depend on hydrostatic pressure. To disentangle the effects of changes in shear stress and transmural pressure, we devised scaffolds that resulted in regions of different shear, but similar transmural pressure, in the same vessel. In some cases, we placed nonvascularized empty channels near a vessel to reduce transmural pressure to zero. Our data indicated that shear stress was the main controller of barrier function; vessels that were exposed to shears above 10–15 dyn/cm² were leakproof. Transmural pressure, however, was the main direct controller of vascular stability, and we found that transmural pressure needed to be positive to obtain stable vessels.

These findings imply that high flow affects stability in two complementary ways: First, by inducing high transmural pressure, high flow directly stabilizes vessels. Second, by inducing high shear, high flow eliminates leaks, and thereby allows a positive transmural pressure to be maintained.

These mechanistic insights, along with those obtained from cAMP-elevation studies, are summarized in [Figure 8.3](#). Note that leaky vessels tend to be unstable, and we believe this correlation holds in general (see [Section 8.6.1](#) for another example). Long-term perfusion in vascularized microfluidic scaffolds is aided by good vascular barrier function.

8.4 Design considerations

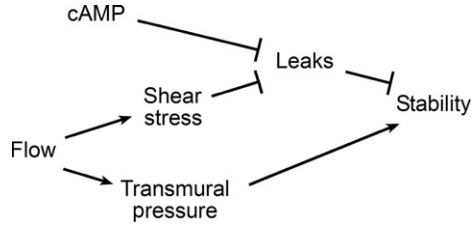
To complement the experimental studies described earlier, we have initiated computational modeling of the transport within vascularized microfluidic scaffolds [24,25]. Here, the goal is to provide straightforward algorithms to design microfluidic scaffolds for a desired outcome. In particular, we would like to design these scaffolds so that perfusion of the vessels can maintain the oxygen concentration within the scaffold and transmural pressure at the vessel surface above their respective thresholds. These thresholds can be measured experimentally; for transmural pressure, the threshold will depend on the contractility of the endothelium and the adhesive strength between endothelium and scaffold, as shown by [Eq. \(8.1\)](#).

8.4.1 Perfusion

When analyzing the perfusion properties of a specific microfluidic scaffold, we not only wish to know whether the network geometry is sufficient for oxygen

-
- ◀ vessels. *Right*, representative images of vessels under long-term perfusion. Dotted lines indicate walls of the collagen channels. (C) Increases in cAMP levels reduce the number of leaks observed in the vessel wall. *Right*, fluorescence images of vessels perfused with 0 or 80 μM db-cAMP. Asterisks indicate locations of leaks. (D) Increases in luminal flow rate reduce the leakiness of the vessel wall.

Source: Modified from Refs. [16,17] with permission from Elsevier.

**FIGURE 8.3**

Mechanisms that affect the mechanical stability of the vessel wall. Arrows (\rightarrow) indicate positive interactions. Perpendicular segments (\perp) indicate inhibitory interactions.

transport, but also to determine which designs are “better” than others. For instance, inflating the diameter of a vessel (e.g., 1 mm) would certainly lead to extremely large fluid flows and large oxygen transfer coefficients. Such a vascular configuration, however, seems artificial to us. It is important to choose an optimizing function that does not lead to extreme vascular designs. Among the various optimizing functions that we have considered include vascular volume fraction (i.e., the fraction of the tissue that consists of vessel lumen), efficiency of oxygen extraction (i.e., ratio of outflow to inflow oxygen concentration), and perfusion power. A vascular design is considered better if it leads to lower vascular volume fraction, higher oxygen extraction efficiency, or lower perfusion power. In all cases, we constrain the driving perfusion pressures at the inlets and outlets of the scaffold.

As a first step, we have analyzed the effectiveness of oxygen transport in a parallel hexagonal array, since the many symmetry planes in this model enable reduction of the computational geometry [25]. In this work, we used vascular volume fraction as the optimizing function. Fluid flow within the lumens was governed by the steady-state Navier–Stokes equations:

$$\rho(\mathbf{v}_{\text{vessel}} \cdot \nabla) \mathbf{v}_{\text{vessel}} = \eta \nabla^2 \mathbf{v}_{\text{vessel}} - \nabla P_{\text{vessel}} \quad (8.2)$$

Fluid flow within the scaffold obeyed Darcy’s law:

$$\mathbf{v}_{\text{scaffold}} = -K \nabla P_{\text{scaffold}} \quad (8.3)$$

The two flows were coupled at the vascular surface by Starling’s law for the filtration velocity (neglecting oncotic terms):

$$v_n = L_p (P_{\text{vessel}} - P_{\text{scaffold}}) \quad (8.4)$$

Finally, transport of oxygen within the lumen and in the scaffold was governed by steady-state reaction–convection–diffusion equations:

$$\mathbf{v}_{\text{scaffold}} \cdot \nabla c_{\text{scaffold}} = D_{\text{O}_2} \nabla^2 c_{\text{scaffold}} - q_{\text{O}_2} \quad (8.5)$$

$$\mathbf{v}_{\text{vessel}} \cdot \nabla c_{\text{vessel}} = D_{\text{O}_2} \nabla^2 c_{\text{vessel}} \quad (8.6)$$

Here, ρ and η are the density and viscosity of the perfusate; $\mathbf{v}_{\text{vessel}}$ and $\mathbf{v}_{\text{scaffold}}$, P_{vessel} and P_{scaffold} , and c_{vessel} and c_{scaffold} are the fluid velocities, fluid pressures, and oxygen concentrations in the vessels and scaffold; K is the hydraulic conductivity of the scaffold; L_p is the endothelial hydraulic conductivity; D_{O_2} is the oxygen diffusivity, and q_{O_2} is the oxygen consumption rate per volume of scaffold.

Each combination of vessel diameter and spacing yielded a minimum oxygen concentration in the scaffold. Using a parametric sweep, we systematically found combinations for which the minimum oxygen concentration equaled a set threshold (5% O_2). Of these combinations, the one that had the lowest vascular volume fraction was designated the optimal design. By altering the other set points in the model (scaffold thickness, oxygen consumption rate, etc.), we found optimal designs as a function of various parameters (Figure 8.4).

Surprisingly, the optimal vessel diameters were on the order of $\sim 100 \mu\text{m}$, which is much larger than the diameters of capillaries *in vivo*. Thus, for perfusion of engineered tissues, it may not be necessary to replicate the exact geometry and scale of vascular beds *in vivo*. We note that $\sim 100\text{-}\mu\text{m}$ diameter vessels can be formed using needle-, gelatin-, or perturbant-based microfluidic scaffolds, so experimental tests of these models are possible.

The unusually symmetric vascular geometry suggested that approximate analytical solution may be possible. When we neglected all axial diffusion of oxygen, filtration and interstitial flow, analytical optimization yielded the following implicit expressions for the optimal diameter D and spacing H :

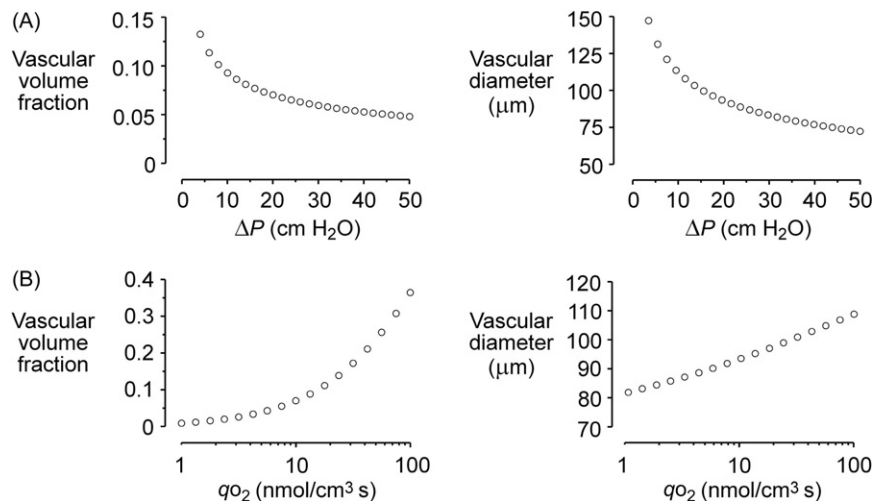
$$\frac{\alpha}{2} - \frac{2\beta L}{\alpha} \left[\left(\frac{H}{D} \right)^2 - 1 \right] \left\{ \beta \gamma \left[\left(\frac{H}{D} \right)^2 - 1 \right] + \delta \left[\left(\frac{H}{D} \right)^2 \ln \left(\frac{H}{D} \right)^2 - \left(\frac{H}{D} \right)^2 + 1 \right] \right\} = 0 \quad (8.7)$$

$$D^2 = \frac{8\beta L}{\alpha} \left[\left(\frac{H}{D} \right)^2 - 1 \right] \quad (8.8)$$

Here, L is the scaffold thickness, whereas α , β , γ , and δ are functions of the remaining parameters (perfusion pressures, inlet oxygen concentration, etc.) (see Ref. [25] for more details). Comparisons of the approximate optima with the computationally determined ones showed agreement to within 5% in nearly all cases. We propose to use these expressions in the rational design of microfluidic scaffolds for perfusion of tissues (see Section 8.5).

8.4.2 Drainage

Our experimental work has shown that transmural pressure must exceed a threshold value for vessels to be stable against delamination from the scaffold. To promote vascular stability, we must find ways to control transmural pressure in a

**FIGURE 8.4**

(A) The effect of perfusion pressure on optimal volume fraction and vessel diameter.
 (B) The effect of oxygen consumption rate per volume on optimal volume fraction and vessel diameter.

Source: Modified from Ref. [25] with permission from the American Institute of Physics.

vascularized scaffold. Since the pressures in the vessels are largely preset by perfusion pressures, the primary way to alter transmural pressure is to control the pressure within the scaffold (P_{scaffold}). We have analyzed the ability of nonvascularized empty channels (“drains”) within the scaffold to modulate scaffold pressure and thereby maintain transmural pressure [24].

As with the models of perfusion, we considered a hexagonal array of vessels. Here, however, we computationally switched a subset of vessels to drains by deleting the endothelium and by setting the inlet and outlet pressures to a drainage pressure (lower than the perfusing pressures) (Figure 8.5A). Although such a vascularized, drained scaffold would be difficult to form experimentally—it would be easier if the drains were all perpendicular to the vessels—this model of parallel vessels and drains has the advantage of computational tractability.

Since we did not consider oxygen transport in these models, the equations to be solved were Eqs. (8.2)–(8.4), with the hydraulic conductivity L_P made infinite at the walls of the drainage channel. For each set of parameters (perfusion pressures, drainage pressure, etc.), we calculated the lowest transmural pressure in the model (Figure 8.5B). Instead of optimizing the drainage design (e.g., by finding the lowest drainage volume fraction that maintained transmural pressure above a threshold), we wanted to determine if simplifying design rules existed. In particular, would it be possible to treat a drain as if it had a “radius-of-action”, within which all vessels would have transmural pressure above threshold and thus be stable?

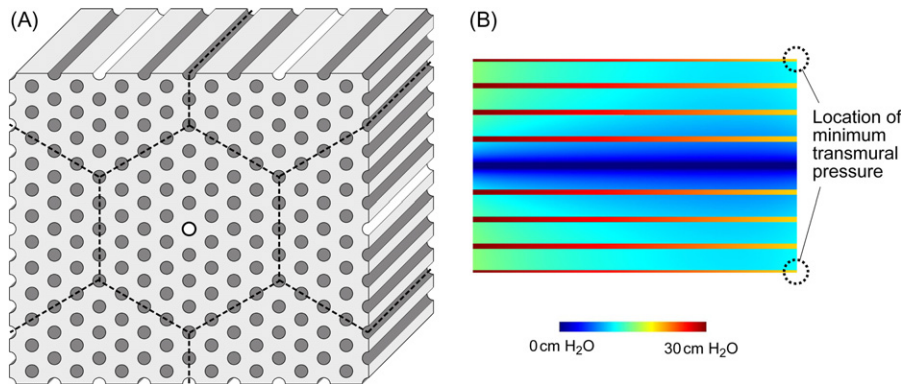


FIGURE 8.5

(A) Cutaway view of a perfused tissue construct with drainage channels. Vessels are gray, while drainage channels are white. Dashed lines represent planes of symmetry that can be exploited during computational analysis. (B) Cross-sectional map of interstitial pressure and luminal pressure in a representative tissue construct. The drainage channel is in the middle, with four vessels on either side. Flow is from left to right. The circle denotes the point of minimum transmural pressure (8.7 cm H₂O in this model).

Source: Modified from Ref. [24] with permission from Elsevier.

We found that it is always possible (e.g., by lowering the drainage pressure) to cause transmural pressure to meet a threshold value for any given vascular and drainage configuration. Moreover, for large ratios of numbers of vessels to drains, the transmural pressure profile becomes a function of the distance from the drain only. For small ratios of numbers of vessels to drains (i.e., a high density of drainage channels), however, interactions between drains raises the overall transmural pressure; in a sense, having more drains increases their radii-of-action.

We found that the effectiveness of a drain in increasing transmural pressure depends largely on the vascular surface area per volume of scaffold, rather than on the individual vascular geometric parameters *per se*. This result allows one to decouple the design of perfusion and drainage systems, in that a given perfusion network (which may have a complex interconnected geometry) can be analyzed for drainage by considering an equivalent parallel vascular array with the same surface area per volume. This result also implies that the relative orientation of drains and vessels is not critical in determining whether drainage is sufficient.

8.5 Design algorithm

We wish to unify these experimental and computational results to answer the following question: Given a particular scaffold and desired seeding density

(and, thus, oxygen consumption rate), how does one design the microfluidic geometry of the scaffold to enable long-term perfusion upon vascularization? Our proposed design algorithm consists of the following steps:

1. Determine or select the threshold oxygen concentration and threshold transmural pressure desired in the scaffold.
2. Choose reasonable perfusion pressures (e.g., 40 cm H₂O at the inlet and 20 cm H₂O at the outlet) and use Eqs. (8.7) and (8.8) to calculate optimal vessel diameters and spacings that maintain oxygen concentration in the scaffold above threshold.
3. From the optimized vascular geometry and chosen perfusion pressures, calculate the shear stress in the vessels. If it is above $\sim 10\text{--}15$ dyn/cm², then the scaffolds can be perfused without leaks. If the shear stress is below this threshold, then special care must be taken to ensure that the vessels do not leak under perfusion (e.g., by supplementing the perfusate with large amounts of cAMP-elevating compounds).
4. Use computational models to determine the maximum drainage spacing for a chosen drainage pressure (e.g., 0 cm H₂O) so that transmural pressure is above threshold. We have found computationally that drainage diameter is only a weak determinant of drainage capacity.

It is important to note that this algorithm yields designs with no built-in safety margin. In general, using more vessels will always improve the perfusion capacity, at the cost of increasing vascular volume fraction; for a given vascular design, using more drains will always improve the drainage capacity. Likewise, this algorithm offers a specific class of microfluidic designs, in which the vessels are parallel and evenly spaced, as are the drains. If more complex geometries (e.g., highly interconnected networks) are desired, then the algorithm can be used to generate starting points for the vascular and drainage design.

8.6 Summary

This chapter summarizes our work to date on forming, vascularizing, and optimizing microfluidic hydrogels for use as tissue scaffolds. Microfluidic scaffolds represent a promising new class of biomaterials that has the potential to directly address the issue of tissue vascularization. We have developed methods to form microfluidic ECM gels, and some of these methods should be suitable for polysaccharide or synthetic polymer gels.

By studying the properties of single vessels (made from scaffolds that contain a single channel), we have deduced several guiding principles for stable vascularization. First, leaks can cause eventual delamination of the vessel wall from the scaffold. Second, delamination is consistent with a physical process governed by an excess of destabilizing over stabilizing stresses. Third, signals that eliminate leaks (high cAMP levels, high shear stress) favor stable perfusion. Fourth, transmural pressure must exceed a threshold value to maintain stability.

By programming these principles into computational models, we have developed an algorithm for microfluidic design. It is important to ensure not only that perfusion is sufficient to maintain tissue viability, but also that drainage is sufficient to maintain vascular stability. We have obtained approximate analytical expressions that yield optimal vascular geometries for perfusion. For drainage, at best we can reduce the computational geometry to a simpler one that contains parallel channels.

8.6.1 Future directions

What obstacles remain toward application of microfluidic scaffolds in tissue reconstruction? Below, we list those we feel are most critical:

First, these experimental methods should be extended to other materials of biomedical interest. We think fibrin gels, alginates, and polyethylene glycol gels represent good places to explore, especially if analyzed in clinically approved formulations.

Second, the studies should make use of more than just endothelial cells. Although endothelial tubes and networks may provide the bare minimum for perfusion with blood, it would be beneficial to incorporate pericytes or smooth muscle cells into the vessel wall. Likewise, the presence of oxygen-consuming parenchymal cells may alter the sensitivity of the vessel wall to cAMP, shear stress, or transmural pressure, so measurements of these thresholds in scaffolds that contain both vascular and nonvascular cells is essential.

Third, the network design should be limited to a small number of inlets and outlets. This requirement will help to make surgical anastomosis practical; in clinical reconstructive surgery, the grafted tissue typically has just a pair of feeding vessels. Probably the simplest way to organize such designs is to make them modular, by coupling treelike portions to an exchange region that consists of parallel arrays of vessels. Computational models should help greatly in predicting which microfluidic designs are appropriate.

New ways to stabilize vessels in microfluidic scaffolds are also welcome. Perfusion with whole blood may reveal cell-borne factors that aid in perfusion. We have identified the macromolecular content of the perfusate as an additional stabilizing factor [26]. It would be helpful to obtain a broad set of stabilizing signals that would provide the experimentalist with some freedom in selecting the most practical way to perfuse a vascularized microfluidic scaffold.

Acknowledgments

This work was supported by the National Institute of Biomedical Imaging and Bioengineering under grant EB005792 and the National Heart, Lung, and Blood Institute under grant HL092335.

References

- [1] Z. Lokmic, G.M. Mitchell, Engineering the microcirculation, *Tissue Eng. B* 14 (2008) 87–103.
- [2] M. Lovett, K. Lee, A. Edwards, D.L. Kaplan, Vascularization strategies for tissue engineering, *Tissue Eng. B* 15 (2009) 353–370.
- [3] R.K. Khouri, Avoiding free flap failure, *Clin. Plast. Surg.* 19 (1992) 773–781.
- [4] C.M. Nelson, J. Tien, Microstructured extracellular matrices in tissue engineering and development, *Curr. Opin. Biotechnol.* 17 (2006) 518–523.
- [5] A.P. Golden, J. Tien, Fabrication of microfluidic hydrogels using molded gelatin as a sacrificial element, *Lab Chip* 7 (2007) 720–725.
- [6] G.M. Price, K.K. Chu, J.G. Truslow, M.D. Tang-Schomer, A.P. Golden, J. Mertz, et al., Bonding of macromolecular hydrogels using perturbants, *J. Am. Chem. Soc.* 130 (2008) 6664–6665.
- [7] R. Montesano, L. Orci, P. Vassalli, *In vitro* rapid organization of endothelial cells into capillary-like networks is promoted by collagen matrices, *J. Cell Biol.* 97 (1983) 1648–1652.
- [8] A.F. Black, F. Berthod, N. L’Heureux, L. Germain, F.A. Auger, *In vitro* reconstruction of a human capillary-like network in a tissue-engineered skin equivalent, *FASEB J.* 12 (1998) 1331–1340.
- [9] M. Radisic, L. Yang, J. Boublik, R.J. Cohen, R. Langer, L.E. Freed, et al., Medium perfusion enables engineering of compact and contractile cardiac tissue, *Am. J. Physiol. Heart Circ. Physiol.* 286 (2004) H507–H516.
- [10] K.M. Chrobak, D.R. Potter, J. Tien, Formation of perfused, functional microvascular tubes *in vitro*, *Microvasc. Res.* 71 (2006) 185–196.
- [11] G.M. Price, J. Tien, Subtractive methods for forming microfluidic gels of extracellular matrix proteins, in: S.N. Bhatia, Y. Nahmias (Eds.), *Microdevices in Biology and Engineering*, Artech House, Boston, MA, 2009, pp. 235–248.
- [12] M.D. Tang, A.P. Golden, J. Tien, Molding of three-dimensional microstructures of gels, *J. Am. Chem. Soc.* 125 (2003) 12988–12989.
- [13] A. Krogh, The number and distribution of capillaries in muscles with calculations of the oxygen pressure head necessary for supplying the tissue, *J. Physiol.* 52 (1919) 409–415.
- [14] D.T. Chiu, N.L. Jeon, S. Huang, R.S. Kane, C.J. Wargo, I.S. Choi, et al., Patterned deposition of cells and proteins onto surfaces by using three-dimensional microfluidic systems, *Proc. Natl. Acad. Sci. U.S.A.* 97 (2000) 2408–2413.
- [15] G.M. Price, J. Tien, Methods for forming human microvascular tubes *in vitro* and measuring their macromolecular permeability, in: A. Khademhosseini, K.-Y. Suh, M. Zourob (Eds.), *Biological Microarrays (Methods in Molecular Biology)*, vol. 671, Humana Press, Totowa, NJ, 2011, pp. 281–293.
- [16] K.H.K. Wong, J.G. Truslow, J. Tien, The role of cyclic AMP in normalizing the function of engineered human blood microvessels in microfluidic collagen gels, *Biomaterials* 31 (2010) 4706–4714.
- [17] G.M. Price, K.H.K. Wong, J.G. Truslow, A.D. Leung, C. Acharya, J. Tien, Effect of mechanical factors on the function of engineered human blood microvessels in microfluidic collagen gels, *Biomaterials* 31 (2010) 6182–6189.

- [18] Z.M. Goeckeler, R.B. Wysolmerski, Myosin light chain kinase-regulated endothelial cell contraction: the relationship between isometric tension, actin polymerization, and myosin phosphorylation, *J. Cell Biol.* 130 (1995) 613–627.
- [19] Z.M. Goeckeler, R.B. Wysolmerski, Myosin phosphatase and cofilin mediate cAMP/cAMP-dependent protein kinase-induced decline in endothelial cell isometric tension and myosin II regulatory light chain phosphorylation, *J. Biol. Chem.* 280 (2005) 33083–33095.
- [20] X. Cullere, S.K. Shaw, L. Andersson, J. Hirahashi, F.W. Lusinskas, T.N. Mayadas, Regulation of vascular endothelial barrier function by Epac, a cAMP-activated exchange factor for Rap GTPase, *Blood* 105 (2005) 1950–1955.
- [21] M.J. Lorenowicz, M. Fernandez-Borja, M.R.H. Kooistra, J.L. Bos, P.L. Hordijk, PKA and Epac1 regulate endothelial integrity and migration through parallel and independent pathways, *Eur. J. Cell Biol.* 87 (2008) 779–792.
- [22] S.-J. Lin, K.-M. Jan, G. Schuessler, S. Weinbaum, S. Chien, Enhanced macromolecular permeability of aortic endothelial cells in association with mitosis, *Atherosclerosis* 73 (1988) 223–232.
- [23] S.-J. Lin, K.-M. Jan, S. Chien, Role of dying endothelial cells in transendothelial macromolecular transport, *Arteriosclerosis* 10 (1990) 703–709.
- [24] J.G. Truslow, G.M. Price, J. Tien, Computational design of drainage systems for vascularized scaffolds, *Biomaterials* 30 (2009) 4435–4443.
- [25] J.G. Truslow, J. Tien, Perfusion systems that minimize vascular volume fraction in engineered tissues, *Biomicrofluidics* 5 (2011) 022201.
- [26] A.D. Leung, K.H.K Wong, J. Tien, Plasma expanders stabilize human microvessels in microfluidic scaffolds, *J. Biomed. Mater. Res. A* 100 (2012) 1815–1822.